THE JOURNAL OF BIOLOGICAL CHEMISTRY VOL. 287, NO. 39, pp. 33094–33103, September 21, 2012

Betaine Homocysteine Methyltransferase Is Active in the Mouse Blastocyst and Promotes Inner Cell Mass Development*

Received for publication, March 22, 2012, and in revised form, July 20, 2012 Published, JBC Papers in Press, July 30, 2012, DOI 10.1074/jbc.M112.365478

Martin B. Lee[‡§1], Megan Kooistra[‡], Baohua Zhang[‡2], Sandy Slow[¶], Amanda L. Fortier[‖3,4], Timothy A. Garrow[‡‡], Michael Lever[¶], Jacquetta M. Trasler[‖**§§¶¶4,5], and Jay M. Baltz[‡§‖‖6]**

*From the [‡]Ottawa Hospital Research Institute, Ottawa, Ontario K1Y4E9, Canada, the [‖‖]Department of Obstetrics and Gynecology (Division of Reproductive Medicine), University of Ottawa Faculty of Medicine, Ottawa, Ontario K1H8L6, Canada, the [§]Department of Cellular and Molecular Medicine, University of Ottawa Faculty of Medicine, Ottawa, Ontario K1H8M5, Canada, the [¶]Biochemistry Unit, Canterbury Health Laboratories, Christchurch 8140, New Zealand, the [‡‡]Department of Food Science and Human Nutrition, University of Illinois, Urbana, Illinois 61801, the [‖]Research Institute of the McGill University Health Centre at the Montréal Children's Hospital, Montréal, Quebec H3H1P3, Canada, the **Department of Human Genetics, McGill University, Montréal, Quebec H3A1B1, Canada, the [§§]Department of Pediatrics, McGill University, Montréal, Quebec H3H1P3, Canada, and the [¶¶]Department of Pharmacology and Therapeutics, McGill University, Montréal, Quebec H3G1Y6, Canada*

Background: Blastocyst stage embryos require a large pool of methyl groups, but the source is unknown.
Results: Betaine-homocysteine methyltransferase (BHMT), which takes methyl groups from betaine, is highly active in mouse blastocysts and promotes development of cells that become the fetus.
Conclusion: BHMT contributes to the methyl pool in the blastocyst.
Significance: Betaine and BHMT promote embryo development.

Methyltransferases are an important group of enzymes with diverse roles that include epigenetic gene regulation. The universal donor of methyl groups for methyltransferases is *S*-adenosylmethionine (AdoMet), which in most cells is synthesized using methyl groups carried by a derivative of folic acid. Another mechanism for AdoMet synthesis uses betaine as the methyl donor via the enzyme betaine-homocysteine methyltransferase (BHMT, EC 2.1.1.5), but it has been considered to be significant only in liver. Here, we show that mouse preimplantation embryos contain endogenous betaine; *Bhmt* mRNA is first expressed at the morula stage; BHMT is abundant at the blastocyst stage but not other preimplantation stages, and BHMT activity is similarly detectable in blastocyst homogenates but not those of two-cell or morula stage embryos. Knockdown of BHMT protein levels and reduction of enzyme activity using *Bhmt*-specific antisense morpholinos or a selective BHMT inhibitor resulted in decreased development of embryos to the blastocyst stage *in vitro* and a reduction in inner cell mass cell number in blastocysts. The detrimental effects of BHMT knockdown were fully rescued by the immediate methyl-carrying product of BHMT, methionine. A physiological role for betaine and BHMT in blastocyst viability was further indicated by increased fetal resorption following embryo transfer of BHMT knockdown blastocysts *versus* control. Thus, mouse blastocysts are unusual in being able to generate AdoMet not only by the ubiquitous folate-dependent mechanism but also from betaine metabolized by BHMT, likely a significant pool of methyl groups in blastocysts.

Preimplantation mammalian embryos develop from fertilized eggs through a series of cleavages until forming the morula, where cell-cell adhesion and functional gap junctions first appear. The final stage of mammalian embryogenesis before implantation in the uterus is the blastocyst, which arises from the morula through a process that includes formation of the fluid-filled blastocoel cavity and differentiation of the initial two cell lineages as follows: the inner cell mass (ICM)[7] and the trophectoderm (1). The trophectoderm is a spherical shell of simple epithelium that encloses the blastocoel and gives rise to the fetal portion of the placenta. The ICM lies at one pole inside the blastocoel cavity enclosed by the trophectoderm and is composed of epiblast progenitors, which are the source of all tissues of the fetus, and primitive endoderm progenitors that will give rise to extraembryonic membranes (2, 3).

At the blastocyst stage, the embryo transitions from a state of low to high metabolic activity, which is accompanied by the expression of genes for components of many biochemical pathways (4). One important class of enzymes is the methyltrans-

* This work was supported in part by Canadian Institutes of Health Research Operating Grant MOP97972 (to J. M. B. and J. T.).
[1] Supported in part by the Program on Oocyte Health funded by Canadian Institutes of Health Research Institute of Human Development Child and Youth Health Strategic Initiative Grant HGG62293.
[2] Supported by a Lalor Foundation postdoctoral fellowship.
[3] Recipient of a Canadian Institutes of Health Research studentship.
[4] Member of the Research Institute of the McGill University Health Centre, which is supported in part by the Fonds de la Recherche en Santé du Québec.
[5] James McGill Professor of McGill University.
[6] To whom correspondence should be addressed: Ottawa Hospital Research Institute, 725 Parkdale Ave., Ottawa, Ontario K1Y 4E9, Canada. Tel.: 613-798-5555 (Ext. 13714); E-mail: jmbaltz@ohri.ca.

[7] The abbreviations used are: ICM, inner cell mass; BHMT, betaine-homocysteine methyltransferase; MT, methyltransferases; AdoMet, *S*-adenosylmethionine; ANOVA, analysis of variance; CBHcy, γ-carboxybutyl homocysteine; hCG, human chorionic gonadotropin; THF, tetrahydrofolate.

ferases (MT) that catalyze the transfer of methyl groups to a vast array of substrates and that are estimated to comprise about 1% of genes in mammals (5). Examination of gene array data (4) indicates that the number of established or putative MT whose mRNAs were detected is ~40 in one-cell embryos and ~60 in blastocysts, implying that an array of MT may function in preimplantation embryos and require an available methyl pool.

The universal methyl donor for almost all MT is *S*-adenosylmethionine (AdoMet) (6). AdoMet is synthesized by the methylation of homocysteine to produce methionine that is then converted to AdoMet by the addition of adenosine and is stored to serve as a labile methyl pool (7). In mammals, homocysteine can be methylated via two pathways. In the pathway operating in most somatic cells, a methyl group derived from serine is carried by folic acid (as methyltetrahydrofolate) and transferred to homocysteine. An alternative pathway utilizes betaine (glycine betaine, *N,N,N*-trimethylglycine). Here, a methyl group is transferred directly from betaine to homocysteine by the enzyme betaine-homocysteine methyltransferase (BHMT; EC 2.1.1.5). The betaine-dependent pathway of AdoMet synthesis has generally been considered to be restricted to liver and possibly also kidney in humans but not in rodents (7, 8).

One key role of MT-mediated methylation during preimplantation embryogenesis is in epigenetic gene regulation and cell fate determination. The best-studied mechanism of epigenetic regulation is DNA methylation of cytosines. Nearly all gamete-specific DNA methylation is erased early in preimplantation embryogenesis. Global embryo-specific *de novo* DNA remethylation then begins at the blastocyst stage, beginning preferentially in the ICM (9–12). Methylation of histone tails on several lysine residues is also an important means of epigenetic control of gene expression, with histone methylation patterns changing during preimplantation development, including increased methylation at the blastocyst stage on residues promoting gene expression (13–15). In addition, arginine methylation on histone H3 reportedly directs embryo blastomeres into the ICM lineage in blastocysts (16). The establishment of such epigenetic markers during embryogenesis is vital for subsequent fetal development.

The source of methyl groups in preimplantation embryos is largely unknown. Some of the AdoMet required before the blastocyst stage may be derived from endogenous maternal folate, but preimplantation embryos do not appear to be capable of taking up additional folate via transporters (17).[8] In contrast, preimplantation mouse embryos can accumulate considerable amounts of betaine via the SIT1 transporter (encoded by the *Slc6a20a* gene) during the one- and two-cell stages (18, 19). Although betaine may function as an organic osmolyte contributing to cell volume regulation in fertilized eggs (18, 20), another possible function was suggested by examination of gene array data (4), which indicated the presence of a high number of *Bhmt* transcripts at the morula stage. Thus, we hypothesized that betaine accumulated by mouse embryos could serve as a substrate for BHMT during preimplantation embryogenesis, contributing to the pool of methyl groups available for MT.

[8] M. Kooistra and J. M. Baltz, unpublished data.

EXPERIMENTAL PROCEDURES

Chemicals and Media—Chemicals and components of culture media were obtained from Sigma unless otherwise noted, and those used in media were embryo tested or cell culture grade. The specific BHMT inhibitor, γ-carboxybutyl homocysteine (CBHcy; (*R,S*)-5-(3-amino-3-carboxy-propylsulfanyl)-pentanoic acid), has been described previously and validated (21, 22) and was custom-synthesized by Orbiter (Urbana, IL). CBHcy was added to media from stock solutions in water. Embryo culture media were based on KSOM and Hepes/KSOM (45) media, except that glutamine was omitted and polyvinyl alcohol (1 mg/ml; cold water-soluble, MW 30,000–70,000) was substituted for BSA.

Mouse Oocytes and Embryos—Animal protocols were approved by the Animal Care Committee of the Ottawa Hospital Research Institute. Oocytes and preimplantation embryos were obtained from CF1 (Crl:CF1) or 129 (129S2/SvPasCrlf) female mice (Charles River, St-Constant, Quebec, Canada) as specified. Growing oocytes were obtained from postnatal day 9 female CF1 neonates, and fully grown oocytes and embryos at various stages were obtained from 4- to 7-week-old female CF1 mice, as described previously (19, 23). Except in neonates, superovulation was stimulated with equine chorionic gonadotropin (IU intraperitoneally). For mature ovulated eggs and embryos, ovulation was triggered with human chorionic gonadotropin (hCG, 5 IU intraperitoneally) at ~47 h post-equine chorionic gonadotropin. For embryos, females were caged overnight individually with BDF1 (B6D2F1/Crl) or 129 strain males beginning immediately after hCG administration. Embryos were isolated from the female tract at approximately the following times after hCG injection (in hours): one-cell embryos, 24; two-cell, 44; four-cell, 56; eight-cell, 67; morula, 76; early cavitating blastocysts, 89; and blastocysts, 93. After collection, oocytes and embryos were maintained in KSOM drops under mineral oil in 5% CO_2, air at 37 °C. For some experiments, embryos were cultured from the two-cell stage or eight-cell stage to blastocyst (72 or 48 h in culture, respectively). For determining development to blastocysts after culture, photomicrographs of the embryos were obtained, and the number of blastocysts was scored.

Betaine Measurements—Endogenous betaine was determined in groups of 50 embryos at the stages specified using a method based on fluorescent derivation of betaine with phenanthrenacyl triflate and detection by high performance liquid chromatography, as described previously (19). Embryos were washed seven times in ice-cold medium, and background was determined from a similar volume of the final wash drop. Betaine was quantified by comparison with external standards and reported as pmol/embryo.

RT-PCR and Quantitative RT-PCR—RNA was extracted from three independent sets of oocytes and embryos and from liver as control (RNeasy Micro Kit, Qiagen, Mississauga, Ontario, Canada) and reverse-transcribed (Retroscript Kit, Ambion, Austin, TX). A separate RNA extraction was also done with three additional sets of two-cell and morula stage embryos. Primer pairs were designed (OligoPerfect, Invitrogen) using mouse reference sequences spanning introns and obtained

from Invitrogen. The *Bhmt* amplicon was 218 bp (forward primer, 5′-ATTCCCCTTTGGATTGGAAC-3′; at nucleotides 1060–1079 of NM_016668; reverse, 5′-TGTGCATGTCCAAACCACTT-3′ at nucleotides 1258–1277). Because no gene has been identified that has constant transcript levels at all preimplantation stages, it is not possible to normalize expression to a reference gene. Therefore, mRNA isolation and reverse transcription were validated by confirming the expected expression pattern of the previously established control genes, peptidylprolyl isomerase A (*Ppia*) and Histone H2a family member Z (*H2afz*), using primer pairs that yield 150- and 202-bp amplicons, respectively (24). These control genes were chosen because it was previously shown that their expression is highly stable at a given stage, and their preimplantation expression patterns have been well documented (24). Conventional PCRs (Hotstar Taq polymerase, Qiagen; Mastercycler thermocycler, Eppendorf, Hamburg, Germany) contained 0.1 embryo equivalent of cDNA in 20 μl, starting at 95 °C for 15 min, followed by 40 cycles (94 °C, 60 s; 60 °C, 30 s, and 72 °C, 60 s), and visualized by agarose gel electrophoresis with ethidium bromide. The primers and thermocycle temperatures were identical for quantitative PCR (FastStart DNA MasterPLUS SYBR Green I kit on a LightCycler® 480 System, Roche Applied Science), except that the cycle times were 60, 10, and 15 s. The amount of cDNA in oocyte or embryo samples after reverse transcription was quantified by quantitative PCR using standard curves constructed with serially diluted PCR products extracted from gels whose concentration was determined by absorbance. Conversion to transcript numbers were done using the calculated molecular weight of amplicons.

Morpholino Treatments—An antisense morpholino (*Bhmt*MO1, 5′-GTGCCATCTTTCCGGTGTAGTGAGT-3′) was targeted to the region around the start codon (position underlined) of *Bhmt*. A control morpholino (GTcCCATgTTTgCGGTcTAcTGAGT), synthesized at the same time, had five mismatches (lowercase). A second *Bhmt* antisense morpholino (*Bhmt*MO2, TAGCTGTTCCCAGCAAAGTCTGTGC) was also used for confirming selected results. This morpholino targeted a region at 72–48 nucleotides 5′ from the start codon. Both were designed and supplied by Gene Tools LLC (Philomath, OR). Morpholinos were prepared as 1 mM stocks in water, and Lipofectin™ (Invitrogen) was used to deliver morpholinos into embryos (25). Lipofectin (0.625 μl) was pre-mixed with morpholino stock (20 μl) and allowed to combine for 10 min before addition of 1.26-fold concentrated KSOM to a final volume of 100 μl. Final concentrations were 200 μM morpholino and 6.25 μl/ml Lipofectin in KSOM. Embryos isolated at the eight-cell stage were cultured for 48 h to fully expanded blastocysts in 33-μl drops.

BHMT Protein Detection—For immunofluorescence detection of BHMT in whole-mount embryos, embryos were fixed in 2% formaldehyde in PBS (40 min), permeabilized with 0.1% Triton X-100 in PBS (40 min), and blocked (1 h) in PBS with 2% fetal bovine serum and 20 mg/ml BSA. The anti-BHMT antibody used has been previously described (8). Embryos were incubated with primary antibody (1:500 in blocking solution) at 4 °C overnight and then with secondary antibody (goat anti-rabbit Alexa 488;1:500 in PBS) for 16 h at 4 °C. DNA was stained with DAPI where specified. Where specified, whole-mount fluorescence intensity was quantitated using ImageJ 1.4 (National Institutes of Health, Bethesda, MD) to draw a perimeter enclosing each embryo and determining the average intensity within the enclosed area, expressed in arbitrary units.

For confocal immunofluorescence detection of BHMT, embryos were treated as for whole-mount, except DNA was labeled with 10 μg/ml bisbenzimide (Hoechst 33258) for 10 min at room temperature and F-actin-labeled with Alexa 594-phalloidin 1:20 for 20 min at room temperature, before labeling with the BHMT and secondary antibodies as above.

Western blot analysis for BHMT was performed using anti-BHMT primary antibody (1:500 in 5% nonfat dry milk or 1% BSA as specified, at 4 °C overnight). Secondary antibody was either horseradish peroxidase goat anti-rabbit secondary (1:5000–10,000 for 1 h at room temperature) for detection by ECL (Pierce ECL substrate, Thermo Fisher Scientific, Rockford, IL) or goat anti-rabbit Alexa 488 (1:1000) for fluorescence detection. Where specified, the membranes were stripped and reprobed with anti-GAPDH (Santa Cruz Biotechnology FL-335, 1:200) as a loading control.

BHMT Activity Assay—A previously published BHMT activity assay (26) was modified to allow its use with very small samples, by substituting [*methyl*-^{3}H]betaine for [*methyl*-^{14}C]betaine and increasing the reaction period from 2 to 24 h. The assay is based on detecting the products of transfer of [^{3}H]methyl groups from [^{3}H]betaine to homocysteine, producing a mixture of [^{3}H]dimethylglycine and [^{3}H]methionine. Briefly, embryos (groups of 50 unless otherwise stated) were subjected to three freeze-thaw cycles with vortexing, and then 50 mM phosphate buffer (pH 7.5) with 100 μM β-mercaptoethanol, containing 0.24 μM [*methyl*-^{3}H]betaine as donor and 1 mM DL-homocysteine as acceptor, was added to a final volume of 0.5 ml. BSA (100 μg) was used as a negative control and crude mouse liver homogenate as positive control and for assay validation. Samples were allowed to react overnight (24 h) and flash frozen until assayed. To detect ^{3}H-labeled dimethylglycine and methionine, the reaction mixture was applied to a 2-ml Dowex 1 × 4 (2–400 mesh) column in hydroxide form. Unreacted [*methyl*-^{3}H]betaine was eluted by three sequential washes with 30 ml of milliQ water and discarded. [^{3}H]Methionine and [^{3}H]dimethylglycine reaction products were then eluted by applying 1 ml of 1.5 M HCl. These reaction products were quantified by scintillation counting of 100 μl of eluent. Where specified, the BHMT inhibitor CBHcy was added to the reaction mixture at a 50 μM concentration.

Blastocyst Cell Counting and Lineage Determination—Trophectoderm and ICM cells were distinguished by differential staining, using bisbenzimide (Hoechst 33258) to label all nuclei and propidium iodide to label only nuclei in permeabilized cells. Trophectoderm cells were selectively permeabilized and labeled with propidium iodide by transient exposure to 10% Triton X-100 and 5 mg/ml propidium iodide for less than 10 s and then immediately fixed in 100% ethanol containing 5 mg/ml bisbenzimide and incubated overnight at 4 °C, as described previously (27). Conventional fluorescence microscopy was used to obtain images of each fluorophore in slightly compressed blastocysts, and propidium iodide-positive nuclei

(trophectoderm) and total nuclei (bisbenzimide) were counted using ImageJ with Cell Counter Plugin. The number of ICM cells was taken to be the difference between the two totals for each blastocyst.

OCT4 (*Pou5f1*) Western blots were performed as described above for BHMT, using an OCT4 antibody (mouse monoclonal C-10, Santa Cruz Biotechnology) at 1:200 dilution, and re-probed for GAPDH as a loading control. OCT4 and NANOG immunofluorescence was used for counting ICM (OCT4-positive nuclei) and epiblast cells (NANOG-positive). Blastocysts were co-stained for OCT4 (C-10, Santa Cruz Biotechnology, 1:400) and NANOG (rabbit polyclonal RECRCAB0002P-F, Cosmo Bio, Carlsbad, CA, 1:200), using Alexa 594 goat anti-mouse and Alexa 488 goat anti-rabbit secondary antisera (Invitrogen, 1:400), as described previously (28). Positive nuclei were counted in slightly compressed blastocysts as described above.

Embryo Transfer—Embryos were cultured as described and then transferred into recipients using standard embryo transfer protocols (29). Embryos for transfer were produced in 129 inbred strain females. Surrogate CD1 females at 8–10 weeks of age were mated during their natural estrus cycle with proven vasectomized males to induce pseudopregnancy. A total of 15 expanded blastocysts were transferred into each surrogate recipient mother, 7 into the right uterine horn, and 8 into the left. Recipients were sacrificed on E10.5 to assess fetal development and resorptions.

Data Analysis—Graphs were prepared and data analyzed using Prism 5 (GraphPad, San Diego). Quantitative data were expressed as the means ± S.E. Comparisons between means were made by ANOVA followed by the Tukey Multiple Comparison test (>2 groups were compared) or by Student's two-tailed *t* test (2 groups were compared with equal variances by *F*-test), paired *t* test where appropriate, or Mann-Whitney test (two groups with unequal variances). Comparisons of two proportions were done using Fisher's exact test. $p < 0.05$ was considered significant.

RESULTS

Endogenous Betaine Content of Preimplantation Mouse Embryos—We previously showed that betaine could be specifically transported into one- and two-cell embryos *in vitro* and that betaine is present in the normal environment of these embryos, *i.e.* oviductal fluid (18, 19). Here, we have shown directly that freshly isolated preimplantation embryos contain betaine at every stage examined, from fertilized eggs (one-cell embryos) through blastocysts (Fig. 1). At the blastocyst stage, however, the total betaine content of embryos was significantly lower than in one-cell through eight-cell embryos, indicating a decrease in endogenous betaine content with embryo development past the morula stage. Separate measurements on morulae, cavitating blastocysts, and blastocysts, collected independently from the first set, confirmed the pattern of ~50% decrease from morula to expanded blastocyst (data not shown). Thus, betaine is present in embryos throughout preimplantation development, and the pool becomes depleted at the blastocyst stage.

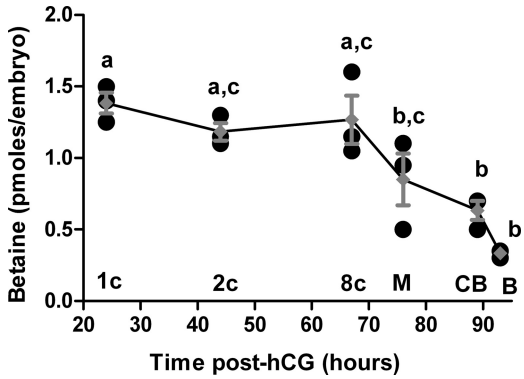

FIGURE 1. **Endogenous betaine in preimplantation embryos.** Total betaine was determined at each stage as indicated (*1c*, one-cell; *2c*, two-cell; *8c*, eight-cell, *M*, morula; *CB*, early cavitating blastocyst; *B*, fully expanded blastocyst), as a function of time post-hCG administration to induce ovulation. Individual measurements ($n = 3$ for each stage) are shown as *black circles*, and means (± S.E.) are shown in *gray*. Means that do not share the same letter are significantly different (ANOVA with Tukey test; $p \leq 0.05$). The one low point at the morula stage is due to a much higher level of background in the wash drop than in any other samples, which was subtracted from the paired measurement. The pre-subtraction measurement was similar to the other two.

Expression of BHMT in Preimplantation Embryos—RT-PCR revealed clear expression of *Bhmt* mRNA beginning around the four-cell stage and continuing through the blastocyst stage (Fig. 2*A*). The identities of representative bands were confirmed by sequencing (data not shown). Quantitative real time PCR revealed that *Bhmt* transcription began at the four-cell stage and peaked at a high level of expression at the morula stage before decreasing at the blastocyst stage (Fig. 2*B*). The *Ppia* expression pattern was essentially as established previously (24). Quantitative PCR on a separately collected set of embryos replicated the increase from very little *Bhmt* expression in two-cell embryos to high expression in morulae (Fig. 2*C*), whereas a different control gene, *H2afz,* chosen because it was reported to have similar expression at these two stages (24), showed no significant change (Fig. 2*C*), confirming that *Bhmt* transcripts were selectively increased.

BHMT protein was detected by Western blot in blastocysts but not in two-cell or morula stage embryos (Fig. 3*A*). Similarly, confocal immunofluorescence of whole-mount embryos showed little staining at the two-cell or morula stages, but intense staining was evident in blastocysts, particularly within the cytoplasm of cells in the ICM as indicated by confocal sections (Fig. 3*B*). This implied that although *Bhmt* transcripts are initiated at the four- to eight-cell stage and peak at the morula stage, translation of *Bhmt* transcripts to BHMT protein occurs in blastocysts.

To confirm that the antiserum used was specific for BHMT in embryos, we knocked down the expression of BHMT in blastocysts using an antisense morpholino (*Bhmt*MO1) directed against *Bhmt*. Blastocysts treated with a control mismatched morpholino exhibited obvious fluorescence by whole-mount immunofluorescence, although a reduction in immunofluorescence was seen with the morpholino targeted against *Bhmt* (Fig. 3*C*). Similarly, Western blots showed that BHMT protein decreased by ~75% in morpholino-treated blastocysts relative to control (Fig. 3*D*). A second, nonoverlapping morpholino directed against *Bhmt* (*Bhmt*MO2) also decreased BHMT

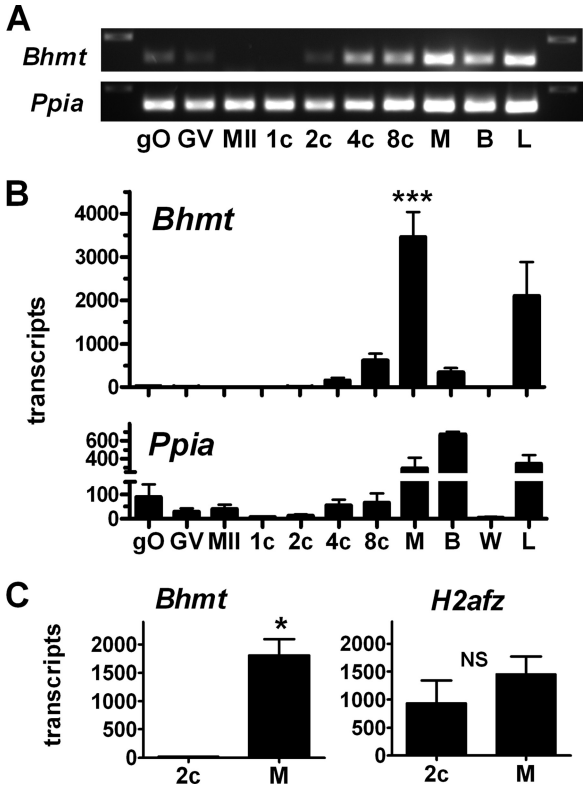

FIGURE 2. **Bhmt mRNA expression in oocytes and preimplantation embryos.** *A,* RT-PCR showing the presence of *Bhmt* mRNA from the four-cell through blastocyst stages, with *Ppia* mRNA as a control. Oocyte stages are as follows: *gO*, growing oocyte; *GV*, germinal vesicle stage; *MII,* mature egg. Preimplantation embryo stages are indicated similarly to Fig. 1. Liver (*L*) served as a positive control. End lanes contained markers (250-bp marker is visible). Identity of representative bands was confirmed by sequencing. *B,* quantitative PCR showing *Bhmt* transcript numbers at each stage of oocyte and preimplantation embryo (*upper graph*), with *Ppia* as a control (*lower graph*). *Bars* represent mean ± S.E. of three independent repeats (*Bhmt*, ***, $p < 0.001$ compared with other stages not including liver; ANOVA with Tukey test). Oocyte and embryo stages are indicated as in *A*; *W* indicates quantitative PCR run with water alone. *C,* quantitative PCR on different two-cell and morula samples ($n = 3$) from those in *B*, confirming significant increase of *Bhmt* transcripts at the morula stage (*left graph*, *, $p = 0.02$ by *t* test) but lack of significant difference ($p = 0.37$, *NS*) in *H2afz* transcripts (*right graph*) between the same samples. *M*, morula;; *B,* fully expanded blastocyst.

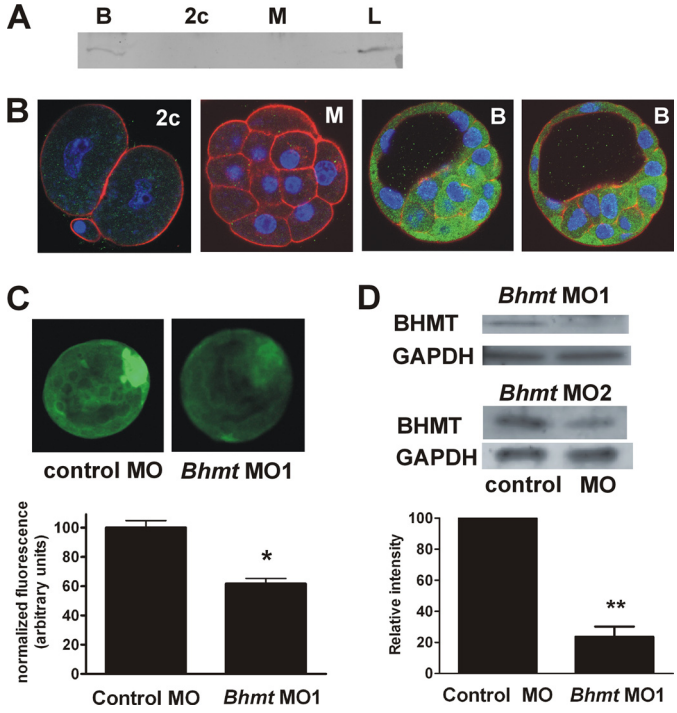

FIGURE 3. **BHMT protein expression and localization in preimplantation embryos.** *A,* Western blot of 200 embryos at the blastocyst (*B*), two-cell (*2c*), and morula (*M*) stages, and 0.5 mg of liver homogenate (*L*). BHMT band is ~45 kDa. *B,* confocal immunofluorescence detection of BHMT. BHMT immunofluorescence in confocal sections of a two-cell embryo (*2c*), a morula (*M*), and two blastocysts (*B*) are shown in *green*, with appreciable signal evident only at the blastocyst stage. DNA (*blue*) was labeled with bisbenzimide (Hoechst 33258) and F-actin (*red*) with phalloidin. The same settings and image adjustments were used for each example. *C,* knockdown of BHMT with morpholino (*MO*). Representative whole-mount conventional immunofluorescence images of BHMT, following culture with *Bhmt*MO1 antisense or control (mismatched) morpholino, are shown at *top* (contrast and intensity were adjusted equally in both images for optimal viewing). Panel at *bottom* shows the fluorescence intensity in arbitrary units normalized to the mean fluorescence in the control group for each of four independent repeats (5–9 per repeat, totals, 22 control; 27 *Bhmt*MO1 antisense). *, $p = 0.027$ for paired *t* test between means of four repeats in each treatment. The fluorescence images shown were chosen to have the approximately same measured intensities as the overall mean fluorescence for each group. *D,* quantitation of BHMT knockdown by Western. Bands from representative gels following culture with *Bhmt*-specific morpholinos are shown at the *top.* The *upper set* shows an example with *Bhmt*MO1 morpholino probed for BHMT above and GAPDH below (59 blastocysts per lane). The *lower set* is with *Bhmt*MO2 morpholino (73 blastocysts per lane). For both, the control is at *left* (mismatched control morpholino for *Bhmt*MO1 or Lipofectin alone for *Bhmt*MO2), and morpholino-treated at *right*, as indicated by labels at *bottom*. The *graph below* shows the mean density of BHMT bands for *Bhmt*MO1-treated blastocysts, each normalized to GAPDH in the same sample. **, $p = 0.007$ by *t* test, $n = 3$ (two Westerns with 59 blastocysts in each lane and one with 64 in each lane). Only the one Western shown was done for *Bhmt*MO2 to confirm knockdown (density normalized to GAPDH was decreased by 65%), and thus no statistical analysis was performed.

expression in blastocysts as assessed by Western blot, with ~65% decrease in intensity *versus* control (Fig. 3*D*).

BHMT Activity—A BHMT activity assay adapted for very small samples was first validated using dilutions of mouse liver homogenate. The generation of labeled products increased with increasing total liver protein, saturating at high protein levels (Fig. 4*A*), with an essentially linear region at lower protein concentrations (Fig. 4*A, inset*). The appearance of labeled product was nearly entirely inhibited by inclusion of the highly selective BHMT inhibitor, CBHcy (21), in the reaction. BHMT activity was apparent in blastocysts, increasing linearly with the number of embryos at least up to 75 (Fig. 4*B*), and lying well within the linear range of the assay as established with liver protein. Groups of 50 blastocysts were thus used in subsequent experiments.

BHMT activity was detected in homogenates of *in vivo*-developed blastocysts, although, in contrast, essentially no activity was detected with equal numbers of morulae (Fig. 4*C*), consistent with the BHMT protein expression pattern (see above). In the presence of the BHMT inhibitor CBHcy, activity in blastocyst homogenate was not significantly different from the apparent activity in an assay containing only BSA instead of homogenate (Fig. 4*D*). Blastocysts that had been cultured from the eight-cell stage in the presence of antisense morpholino (*Bhmt*MO1) directed against *Bhmt* exhibited a significantly reduced activity (Fig. 4*D*). The knockdown of BHMT activity by the *Bhmt* antisense morpholino was ~60–70% (if the level obtained in the presence of CBHcy or with BSA alone is assumed to represent background), paralleling the decrease in BHMT protein levels indicated by Western blots (above). The

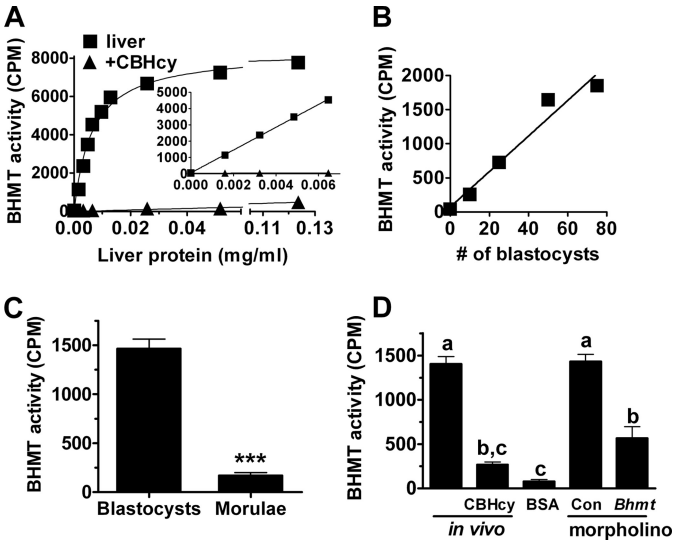

FIGURE 4. **BHMT activity in blastocysts.** *A,* validation of BHMT assay with liver homogenate. Activity is indicated in counts/min of ^{3}H eluted from column, taken to indicate total dimethylglycine and methionine produced. The assay was run in parallel with no inhibitor (*squares*) or CBHcy (50 μM, *triangles*) added. The *inset* shows the pseudolinear region on an expanded scale. The line was fit by linear regression ($r^2 = 0.999$). Each point is the mean of three independent repeats. The *error bars* (S.E.) are not visible because they lie within the symbols. *B,* BHMT activity assay of blastocysts, as a function of blastocyst number (0, 10, 25, 50, and 75). The line was fit by linear regression ($r^2 = 0.956$). *Error bars* (S.E.) lie within the symbols. *C,* comparison of BHMT activity between blastocysts and morulae. *Bars* indicate the means ± S.E. of three repeats (50 morulae or blastocysts each per repeat). ***, $p = 0.0002$ by *t* test. *D,* effect of morpholino (*Bhmt*MO1) on BHMT activity. *Bars* (mean ± S.E.) that do not share the same letter are significantly different (by ANOVA with Tukey test; $n = 3$–5 repeats for each group). Measured activity was not significantly different between blastocysts that had developed *in vivo* and those cultured from the eight-cell stage in the presence of control morpholino (*Con*). The BHMT inhibitor CBHcy decreased measured activity in blastocysts to a level not significantly different from the BSA control ($p < 0.001$, *a versus c*). Activity in blastocysts cultured in the presence of *Bhmt*-specific morpholino *Bhmt*MO1 was significantly decreased ($p < 0.001$, *a versus b*) to a level not significantly different from that with CBHcy.

activity measured for blastocysts that had been cultured with control mismatched morpholino was indistinguishable from that of *in vivo*-developed blastocysts.

Effect of BHMT Knockdown on Blastocyst Development and Cell Lineage Allocation—Fewer eight-cell embryos developed to the blastocyst stage at 72 h when BHMT expression and activity were suppressed with the *Bhmt*MO1 antisense morpholino compared with the mismatched morpholino control (control morpholino, 511/572 embryos = 89.3% *versus* *Bhmt*MO1, 409/601 = 68.1%, in 43 paired cultures; $p < 0.0001$ by Fisher's exact test). The second antisense morpholino, *Bhmt*MO2, similarly decreased development to blastocysts (Lipofectin alone, 100/109 embryos = 91.7% *versus* *Bhmt*MO2, 76/109 = 69.7%, in eight paired cultures, $p < 0.0001$). The majority of embryos, however, progressed to blastocysts with either morpholino.

Because perturbations to preimplantation embryo development can result in changes in the number of cells and their lineage allocations even when blastocysts develop, we used differential staining to determine the numbers of trophectoderm *versus* ICM cells in the blastocysts that developed under each condition. Knocking down the expression of BHMT with *Bhmt*MO1 antisense morpholino did not significantly affect the numbers of trophectoderm cells relative to control morpholino or untreated controls. However, the number of ICM cells was significantly decreased in *Bhmt*MO1 antisense morpholino-treated embryos (Fig. 5*A*), by about 40%. The number of ICM cells was also decreased by *Bhmt*MO2 treatment (Fig. 5*B*), again not affecting trophectoderm cell number (data not shown).

To assess the effects of decreased BHMT activity independently from morpholino treatment, we also cultured embryos from the two-cell stage to blastocysts in the presence of the BHMT inhibitor CBHcy (500 μM added to the medium). The number of embryos reaching the blastocyst stage was decreased in the presence of CBHcy (control, 58/64 = 90.6%; CBHcy, 45/64 = 70.3% embryos; in five paired cultures, $p = 0.007$ by Fisher's exact test). CBHcy treatment also significantly decreased the numbers of ICM cells in blastocysts (Fig. 5*C*) by about 20%.

As a further indication that ICM was decreased, we used Western blots to quantify OCT4 (*Pou5f1*), which is expressed only in the ICM in blastocysts (30), with the assumption that a decrease in the number of OCT4-expressing ICM cells should be reflected by a decrease in total OCT4 per blastocyst. OCT4 protein content was decreased in blastocysts in which BHMT expression was decreased with *Bhmt*MO1 antisense morpholino compared with control morpholino (Fig. 5*D*), consistent with the presence of fewer OCT4-positive ICM cells. OCT4 expression also trended toward a decrease (by ~20%) in CBHcy-treated blastocysts, although this decrease did not reach significance (mean expression relative to control = 80.8 ± 9.6, $n = 5$, $p = 0.1$ by paired *t* test).

We also used immunofluorescence to quantify the numbers of OCT4-positive (ICM), and NANOG-positive (epiblast subset of ICM) nuclei in blastocysts. The number of OCT4-positive nuclei was significantly decreased in blastocysts in which BHMT had been knocked down using *Bhmt*MO2 (Fig. 5*E*). The number of NANOG-positive cells showed a trend toward decreasing, although this did not quite reach significance. Similar results were obtained in embryos cultured with the BHMT inhibitor, CBHcy, where OCT4-positive cells were reduced from a mean of 20.0 ± 0.7 in control to 18.1 ± 0.6 in CBHcy ($p = 0.03$, *t* test), and NANOG-positive cells decreased from 12.0 ± 0.5 to 10.0 ± 0.4 ($p = 0.002$; 55 and 54 embryos in control and CBHcy groups, respectively).

If the decreases in ICM cell number were due to decreased BHMT activity, then the decreases should be rescued by the provision of the immediate product of BHMT, methionine. Exogenous methionine should be effective because it can be taken up by blastocysts and transported into the trophectoderm and ICM (31), and exogenous methionine provided to embryos *in vitro* can be converted to intracellular AdoMet (32). Methionine (0.2 mM), when added to the medium, rescued the development of embryos cultured from the eight-cell stage to blastocysts from the effects of BHMT knockdown by *Bhmt*MO1 morpholino (Fig. 5*F*). Methionine also restored the number of ICM cells when BHMT was knocked down by antisense morpholino to the levels that developed with the control morpholino (Fig. 5*G*).

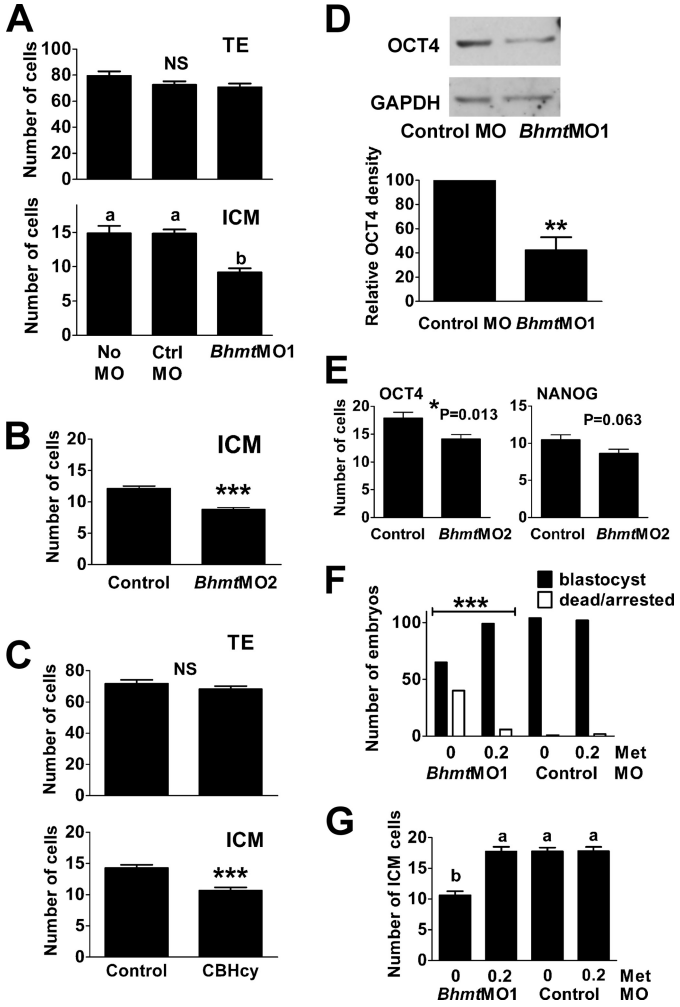

FIGURE 5. **Effect of perturbing BHMT on blastocyst cell allocation.** *A,* effect of BHMT knockdown by *Bhmt*MO1 on blastocyst cell allocation. The *top panel* shows mean trophectoderm (*TE*) cell numbers and the *bottom panel* shows ICM cell numbers for embryos with no morpholino treatment (*no MO*), control morpholino (*Ctrl MO*), and *Bhmt*-specific morpholino (*Bhmt*MO1). The numbers of blastocysts assessed were 29 for no morpholino treatment, 59 for control morpholino, and 65 for *Bhmt*MO1, from at least four independent cultures in each condition. For trophectoderm, *NS* indicates no significant difference among groups by ANOVA ($p = 0.19$). For ICM, $p < 0.001$ for *a versus b* by ANOVA with Tukey test. *B,* effect of *Bhmt*MO2 on ICM cell numbers. The mean ICM cell numbers are shown for control (Lipofectin only) and *Bhmt*MO2 morpholino-treated blastocysts. The number of blastocysts assessed were 35 for morpholino and 50 for control from three separate cultures. ***, $p < 0.0001$ by *t* test. Trophectoderm cell numbers were not significantly different ($p = 0.25$; data not shown). *C,* effect of BHMT inhibitor, CBHcy on blastocyst cell allocation. The *top panel* shows trophectoderm (*TE*) cell numbers and the *bottom panel* shows ICM cell numbers for embryos cultured with no addition (control) or CBHcy (500 μM), as indicated at bottom. The numbers of blastocysts assessed were 37 for control and 43 for CBHcy, from three independent cultures for both treatments. For trophectoderm, *NS* indicates no significant difference among groups ($p = 0.28$), and for ICM, ***, $p < 0.0001$, by *t* test. *D,* effect of BHMT knockdown on OCT4 expression. The *top panel* shows an example of Western blot probed for OCT4 (*upper panel*) and GAPDH (*lower panel*) of blastocysts with control or *Bhmt*-specific morpholino *Bhmt*MO1, quantified in the *bottom panel* as OCT4 normalized in each sample to GAPDH, relative to the expression for the control morpholino in the same experiment set arbitrarily to 100. The *bars* represent the means ± S.E. for five independent repeats. Within each repeat, equal numbers of blastocysts were loaded in each lane (22–30). **, $p = 0.006$ by paired *t* test. In two repeats, embryos cultured with no morpholino were included (data not shown) and had relative band densities of 96 and 144, similar to control morpholino. *E,* effect of BHMT knockdown on numbers of OCT4- and NANOG-positive cells. Panels show mean numbers of OCT4-positive (*left panel*) and NANOG-positive (*right panel*) nuclei in control (Lipofectin only) and *Bhmt*MO2 morpholino-treated blastocysts. The numbers of blastocysts assessed for OCT4 and NANOG were 23 for control and 14 for *Bhmt*MO2, from three independent cultures. An additional four control and seven *Bhmt*MO2 blastocysts were not visibly stained with the OCT4 antibody and were not included. Significance was assessed by *t* test, yielding *p* values indicated within the panels. *F,* rescue of development to the blastocyst stage by methionine added to the medium. Embryos were treated with *Bhmt*MO1 or control morpholino as indicated at bottom, with no (0) methionine (*Met*) or 0.2 mM added. The number of embryos developing to the blastocyst stage (*black*) or arrested or dead (*white*) was scored for eight separate cultures (7–16 embryos per culture, for 104–105 embryos per group) for each condition, and data were pooled. The rescue by methionine on development with *Bhmt* morpholino was highly significant (***, $p < 0.001$ by Fisher's exact test for *Bhmt*MO1 morpholino with methionine *versus* without). *G,* rescue of ICM cell number by methionine. Treatment groups were as in *D*. ICM cell numbers were decreased by *Bhmt*MO1 relative to control in the absence of methionine but were not different from control when methionine (0.2 mM) was present in the medium. 45–50 blastocysts from five independent cultures were assessed per treatment group. $p < 0.001$ for *a versus b* by ANOVA with Tukey test.

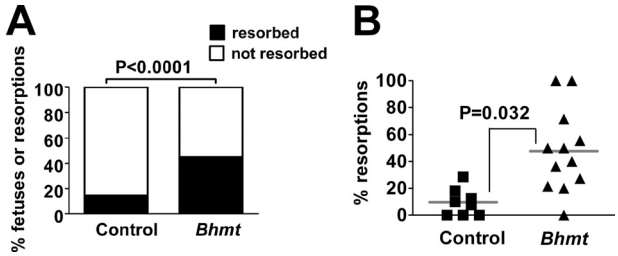

FIGURE 6. **Effect of BHMT knockdown in blastocysts on fetal development on E10.5.** *A,* fetal development on E10.5 after transfer of blastocysts in which BHMT had been knocked down by specific antisense morpholino (*Bhmt*MO1) compared with control morpholino. Pregnancies (fetuses or resorption sites) were found in 12 recipients in the control morpholino group and 14 in the *Bhmt*MO1 morpholino group. Numbers of fetuses and resorptions were pooled for each group and analyzed in a 2×2 table, as recommended (33). The control group had 70 fetuses and 12 resorption sites, and the *Bhmt* morpholino group had 60 fetuses and 49 resorption sites, shown as percentages of the total. The difference was highly significant ($p < 0.0001$) by Fisher's exact test. *B,* alternative analysis by frequency of resorptions in each recipient. For this analysis by recipient, only those recipients that had five or more implantations (fetuses + resorptions) were included (8 out of 12 control morpholino recipients, 12 out of 14 *Bhmt*MO1 morpholino). The means (*horizontal gray lines*) were significantly different ($p = 0.0032$ by Mann-Whitney test, used because variances were significantly different by *F* test, $p = 0.007$).

Effect of BHMT Knockdown in Blastocysts on Subsequent Fetal Development—Embryos were cultured from the eight-cell to blastocyst stages with *Bhmt*MO1 antisense or control mismatched morpholinos, and cohorts of 15 of the resulting blastocysts were transferred to pseudopregnant recipients. Uterine horns were excised on E10.5; resorption sites and fetuses were counted, and the fetuses were removed for further analysis. Pregnancies were established (*i.e.* at least one fetus or resorption on E10.5) in 14 and 12 recipients for the *Bhmt*MO1 antisense and control groups, respectively.

The numbers of fetuses and resorption sites were determined for each pregnant recipient, and data from individual recipients were pooled for analysis as categorical data, as recommended (33). There was no significant difference in the embryo implantation rate in pregnant recipients between treatments (data not shown; $p = 0.13$). The expected low rate of resorptions of ~15% of embryos transferred was observed for the control group (Fig. 6*A*). However, in the *Bhmt* antisense group, the proportion of resorptions was increased to ~45%. This difference was highly significant, indicating a marked increase in spontaneous abortion in fetuses in which BHMT had been knocked down. The significant increase in resorptions in the BHMT knockdown

group was also evident when analyzed by comparing mean resorption rates per individual recipient (Fig. 6*B*). The proportion of fetuses developing per embryo transferred in pregnant recipients was also significantly lower in the BHMT knockdown group (29% *versus* 39%, $p = 0.04$, Fisher's exact test). Among the surviving fetuses, there was no significant difference in crown-rump length between the two groups (5.2 ± 0.1 mm *Bhmt* knockdown *versus* 5.4 ± 0.1 control, $p = 0.25$ by *t* test), nor in somite number, although there may have been a slight trend to lower somite number in the BHMT knockdown group (32.1 ± 0.5 *versus* 33.3 ± 0.4 in control, $p = 0.07$ by *t* test).

DISCUSSION

It was previously established that preimplantation embryos are capable of taking up betaine from their external environment via a specific transporter, SIT1 (18, 19). Here, we showed that betaine accumulation by embryos also likely occurs *in vivo*, because freshly isolated embryos contain betaine at all preimplantation stages. Assuming a cytoplasmic volume of ~180 pl, the endogenous intracellular betaine concentration up to the blastocyst stage is calculated to be ~7 mM. Thus, preimplantation mouse embryos contain betaine at levels similar to the ~4 mM reported as the average over the whole tissue in liver (34), which is the tissue with the highest reported betaine levels, implying that preimplantation mouse embryos contain a substantial stockpile of betaine. The data also clearly indicate that BHMT is active in blastocysts, which implies that accumulated betaine can be utilized as a methyl source at that stage. The evidence for this includes that *Bhmt* mRNA was found to be expressed at a high level in morulae; BHMT protein was specifically detectable in blastocysts, and BHMT enzyme activity was demonstrated there. The observed decrease in endogenous betaine at the blastocyst stage is consistent with betaine being taken up and retained by preimplantation embryos and then metabolized by BHMT expressed only in blastocysts.

BHMT appears to have a physiological role in blastocysts. Cultured embryos in which BHMT was knocked down using either of two nonoverlapping antisense morpholinos developed to blastocysts at decreased rates, and those that developed showed a deficit in ICM cells. An effect of BHMT knockdown mainly on ICM is consistent with the apparent preferential expression of BHMT in that lineage. The detrimental effect of *Bhmt* antisense morpholinos appeared to be specific, because two nonoverlapping *Bhmt* morpholinos had similar effects, and no effect was seen with a control morpholino synthesized at the same time, and the Lipofectin used for loading had no effect by itself. Furthermore, a similar effect on ICM cell numbers was observed in embryos cultured in the presence of the BHMT inhibitor CBHcy. Finally, specificity was supported by the ability of methionine, the immediate methyl-carrying product of BHMT, to fully rescue blastocyst and ICM development in *Bhmt* antisense morpholino-treated blastocysts (although we cannot rule out other effects of methionine, which participates in many biochemical pathways). Together, these data indicated that cultured mouse blastocysts do not develop optimally when BHMT activity is decreased. This was supported by embryo transfer experiments that showed an increased level of fetal resorption when BHMT had been knocked down at the blastocyst stage. The observed effect on fetal development is unlikely to have been due to an effect of morpholino persisting within the cells of the developing embryo after implantation, because intracellular morpholino would be quickly diluted by the rapid increase in total embryo volume and because the lifetime of morpholinos within cells is limited.

In addition to betaine, folate may also have a role in AdoMet generation in preimplantation embryos. Unlike betaine, folate metabolism contributes not only to AdoMet generation but also to purine synthesis. Both AdoMet generation and purine synthesis from folic acid share a common pathway requiring conversion of folic acid to tetrahydrofolate (THF) via the enzyme dihydrofolate reductase but then diverge (35). For AdoMet production, THF is converted to methyl-THF by methyltetrahydrofolate reductase, after which methyl-THF donates its methyl group to homocysteine to generate methionine and then AdoMet (7, 35), converging with the betaine-dependent pathway. O'Neill (17) has shown that inhibition of dihydrofolate reductase with methotrexate blocks mouse embryo development, which could then be rescued by provision of exogenous thymidine, and we have confirmed this,[9] indicating that dihydrofolate reductase is likely active, and tetrahydrofolate is being synthesized. Kwong *et al.* (36) have done similar but more extensive studies in cow and sheep, and they found that methotrexate reduces blastocyst cell number even when exogenous purines and pyrimidines were provided, implying that methyl pool generation may also be affected. Furthermore, mRNA for the enzymes needed for folate-dependent AdoMet generation were shown to be present in bovine embryos (36, 37), as well as in human embryonic stem cells that are analogous to ICM cells (38), also supporting the idea that the folate-dependent pathway is functioning in preimplantation embryos. The relative importance of the folate- and betaine-dependent pathways for AdoMet generation in mouse blastocysts is not known and remains to be investigated. There may also be species differences because, although mouse preimplantation embryos clearly express *Bhmt* mRNA, it is variously reported that bovine preimplantation embryos express *Bhmt* mRNA (37) or that it is lacking (36), whereas human embryonic stem cells express it, as noted above.

Our demonstration here of a detrimental effect on blastocyst development and subsequent fetal viability when BHMT was perturbed in blastocysts *in vitro* contrasts with the recent report (39) of the production of a *Bhmt* knock-out mouse. In that model, $Bhmt^{-/-}$ offspring appeared at a normal Mendelian ratio from heterozygous matings, and matings between $Bhmt^{-/-}$ pairs produced normal litter sizes (39). One possible explanation is that the effect of BHMT depletion on blastocyst and subsequent fetal development produces a clear phenotype only in embryos cultured *in vitro*. There is ample evidence that relatively mild stress restricted to the preimplantation period can result in disruption of epigenetic gene regulation, dysregulation of fetal and placental growth, and increased susceptibility to a range of morbidities in the offspring (40, 41). Thus, a synergistic effect between culture stress and BHMT depletion

[9] B. Zhang and J. M. Baltz, unpublished data.

could result in the phenotype observed. A second possibility is that *Bhmt*$^{-/-}$ embryos could be rescued by methionine that is available in uterine fluid *in vivo* (42), similar to the ability of methionine to rescue ICM cell numbers in BHMT knockdown blastocysts *in vitro*. Third, a differential effect among mouse strains cannot be ruled out, because the embryos used here were from CF1 and 129 strain females, whose embryos are particularly susceptible to culture stress, although the *Bhmt*$^{-/-}$ mice were on a C57Bl/6 background. Finally, the folate-dependent pathway appears to be up-regulated in *Bhmt*$^{-/-}$ and *Bhmt*$^{+/-}$ females, because there was evidence of increased methylfolate utilization in *Bhmt*$^{-/-}$ mice (39). This could result in increased folate accumulated within their embryos. These possibilities remain to be explored and need to be resolved.

The finding that embryos contain large amounts of betaine and that BHMT is active in mouse blastocysts was somewhat surprising, as the utilization of betaine to generate AdoMet has been considered to be specific to liver in rodents. Previous work has shown that betaine is specifically accumulated by preimplantation mouse embryos only at the one- and two-cell stages by the SIT1 transporter that is activated after fertilization, with no further specific uptake through the blastocyst stage (18, 19). At the one- and two-cell stages, betaine has been shown to contribute to normal cell volume regulation, by acting as an organic osmolyte that provides benign intracellular osmotic support to maintain cell size (18, 20, 43). The results reported here indicate that betaine has an additional function and is retained in the embryo until the blastocyst stage, where it is metabolized by BHMT, likely contributing to the cellular store of AdoMet that is the substrate for important MT enzymes, including several that function in epigenetic gene regulation.

Betaine is not a normal component of embryo culture media, including those for humans and domestic species. In experimental systems, however, betaine has been found to promote development of mouse embryos from fertilized eggs (20, 43) and to support a pattern of protein synthesis that more closely resembles that of *in vivo*-produced embryos (44). The results reported here indicate that addition of betaine to embryo culture media can help maintain the methyl pool required for normal embryo development. Thus, addition of betaine to embryo culture media may be beneficial for healthy embryo development *in vitro*.

Acknowledgments—We thank Adriana Gambarotta for expert assistance with embryo transfers and Violetta Siyanov for preparation of a set of embryo samples used for PCR.

REFERENCES

1. Biggers, J. D., Bell, J. E., and Benos, D. J. (1988) Mammalian blastocysts. Transport functions in a developing epithelium. *Am. J. Physiol.* **255,** C419-C432
2. Rossant, J., and Tam, P. P. (2009) Blastocyst lineage formation, early embryonic asymmetries and axis patterning in the mouse. *Development* **136,** 701–713
3. Gasperowicz, M., and Natale, D. R. (2011) Establishing three blastocyst lineages. Then what? *Biol. Reprod.* **84,** 621–630
4. Zeng, F., Baldwin, D. A., and Schultz, R. M. (2004) Transcript profiling during preimplantation mouse development. *Dev. Biol.* **272,** 483–496
5. Katz, J. E., Dlakić, M., and Clarke, S. (2003) Automated identification of putative methyltransferases from genomic open reading frames. *Mol. Cell. Proteomics* **2,** 525–540
6. Loenen, W. A. (2006) *S*-Adenosylmethionine. Jack of all trades and master of everything? *Biochem. Soc. Trans.* **34,** 330–333
7. Selhub, J. (1999) Homocysteine metabolism. *Annu. Rev. Nutr.* **19,** 217–246
8. Delgado-Reyes, C. V., Wallig, M. A., and Garrow, T. A. (2001) Immunohistochemical detection of betaine-homocysteine *S*-methyltransferase in human, pig, and rat liver and kidney. *Arch. Biochem. Biophys.* **393,** 184–186
9. Monk, M., Boubelik, M., and Lehnert, S. (1987) Temporal and regional changes in DNA methylation in the embryonic, extraembryonic, and germ cell lineages during mouse embryo development. *Development* **99,** 371–382
10. Santos, F., Hendrich, B., Reik, W., and Dean, W. (2002) Dynamic reprogramming of DNA methylation in the early mouse embryo. *Dev. Biol.* **241,** 172–182
11. Reik, W., Dean, W., and Walter, J. (2001) Epigenetic reprogramming in mammalian development. *Science* **293,** 1089–1093
12. Santos, F., Zakhartchenko, V., Stojkovic, M., Peters, A., Jenuwein, T., Wolf, E., Reik, W., and Dean, W. (2003) Epigenetic marking correlates with developmental potential in cloned bovine preimplantation embryos. *Curr. Biol.* **13,** 1116–1121
13. Reik, W. (2007) Stability and flexibility of epigenetic gene regulation in mammalian development. *Nature* **447,** 425–432
14. Ooga, M., Inoue, A., Kageyama, S., Akiyama, T., Nagata, M., and Aoki, F. (2008) Changes in H3K79 methylation during preimplantation development in mice. *Biol. Reprod.* **78,** 413–424
15. Liu, H., Kim, J. M., and Aoki, F. (2004) Regulation of histone H3 lysine 9 methylation in oocytes and early pre-implantation embryos. *Development* **131,** 2269–2280
16. Torres-Padilla, M. E., Parfitt, D. E., Kouzarides, T., and Zernicka-Goetz, M. (2007) Histone arginine methylation regulates pluripotency in the early mouse embryo. *Nature* **445,** 214–218
17. O'Neill, C. (1998) Endogenous folic acid is essential for normal development of preimplantation embryos. *Hum. Reprod.* **13,** 1312–1316
18. Anas, M. K., Hammer, M. A., Lever, M., Stanton, J. A., and Baltz, J. M. (2007) The organic osmolytes betaine and proline are transported by a shared system in early preimplantation mouse embryos. *J. Cell Physiol.* **210,** 266–277
19. Anas, M. K., Lee, M. B., Zhou, C., Hammer, M. A., Slow, S., Karmouch, J., Liu, X. J., Bröer, S., Lever, M., and Baltz, J. M. (2008) SIT1 is a betaine/proline transporter that is activated in mouse eggs after fertilization and functions until the two-cell stage. *Development* **135,** 4123–4130
20. Hammer, M. A., and Baltz, J. M. (2002) Betaine is a highly effective organic osmolyte but does not appear to be transported by established organic osmolyte transporters in mouse embryos. *Mol. Reprod. Dev.* **62,** 195–202
21. Collinsova, M., Strakova, J., Jiracek, J., and Garrow, T. A. (2006) Inhibition of betaine-homocysteine *S*-methyltransferase causes hyperhomocysteinemia in mice. *J. Nutr.* **136,** 1493–1497
22. Jiracek, J., Collinsova, M., Rosenberg, I., Budesinsky, M., Protivinska, E., Netusilova, H., and Garrow, T. A. (2006) *S*-Alkylated homocysteine derivatives. New inhibitors of human betaine-homocysteine *S*-methyltransferase. *J. Med. Chem.* **49,** 3982–3989
23. Fitzharris, G., and Baltz, J. M. (2006) Granulosa cells regulate intracellular pH of the murine growing oocyte via gap junctions. Development of independent homeostasis during oocyte growth. *Development* **133,** 591–599
24. Mamo, S., Gal, A. B., Bodo, S., and Dinnyes, A. (2007) Quantitative evaluation and selection of reference genes in mouse oocytes and embryos cultured *in vivo* and *in vitro*. *BMC Dev. Biol.* **7,** 14
25. Siddall, L. S., Barcroft, L. C., and Watson, A. J. (2002) Targeting gene expression in the preimplantation mouse embryo using morpholino antisense oligonucleotides. *Mol. Reprod. Dev.* **63,** 413–421
26. Garrow, T. A. (1996) Purification, kinetic properties, and cDNA cloning of mammalian betaine-homocysteine methyltransferase. *J. Biol. Chem.* **271,** 22831–22838
27. Thouas, G. A., Korfiatis, N. A., French, A. J., Jones, G. M., and Trounson,

A. O. (2001) Simplified technique for differential staining of inner cell mass and trophectoderm cells of mouse and bovine blastocysts. *Reprod. Biomed. Online* **3,** 25–29
28. Igarashi, H., Knott, J. G., Schultz, R. M., and Williams, C. J. (2007) Alterations of PLCβ1 in mouse eggs change calcium oscillatory behavior following fertilization. *Dev. Biol.* **312,** 321–330
29. Hogan, B., Beddington, R., Constantini, F., and Lacy, E. (1994) *Manipulating the Mouse Embryo: A Laboratory Manual*, 2 Ed., pp. 178–181, Cold Spring Harbor Laboratory Press, Cold Spring Harbor, NY
30. Palmieri, S. L., Peter, W., Hess, H., and Schöler, H. R. (1994) Oct-4 transcription factor is differentially expressed in the mouse embryo during establishment of the first two extraembryonic cell lineages involved in implantation. *Dev. Biol.* **166,** 259–267
31. Miller, J. G., and Schultz, G. A. (1985) Amino acid transport in mouse blastocyst compartments. *J. Embryol. Exp. Morphol.* **89,** 149–158
32. Menezo, Y., Khatchadourian, C., Gharib, A., Hamidi, J., Greenland, T., and Sarda, N. (1989) Regulation of *S*-adenosylmethionine synthesis in the mouse embryo. *Life Sci.* **44,** 1601–1609
33. Clark, D. A., Petitbarat, M., and Chaouat, G. (2008) How should data on murine spontaneous abortion rates be expressed and analyzed? *Am. J. Reprod. Immunol.* **60,** 192–196
34. Slow, S., Lever, M., Chambers, S. T., and George, P. M. (2009) Plasma-dependent and -independent accumulation of betaine in male and female rat tissues. *Physiol. Res.* **58,** 403–410
35. Fowler, B. (2001) The folate cycle and disease in humans. *Kidney Int. Suppl.* **78,** S221-S229
36. Kwong, W. Y., Adamiak, S. J., Gwynn, A., Singh, R., and Sinclair, K. D. (2010) Endogenous folates and single-carbon metabolism in the ovarian follicle, oocyte, and pre-implantation embryo. *J. Reprod. Fertil.* **139,** 705–715
37. Ikeda, S., Namekawa, T., Sugimoto, M., and Kume, S. (2010) Expression of methylation pathway enzymes in bovine oocytes and preimplantation embryos. *J. Exp. Zool. A Ecol. Genet. Physiol.* **313,** 129–136
38. Steele, W., Allegrucci, C., Singh, R., Lucas, E., Priddle, H., Denning, C., Sinclair, K., and Young, L. (2005) Human embryonic stem cell methyl cycle enzyme expression. Modeling epigenetic programming in assisted reproduction? *Reprod. Biomed. Online* **10,** 755–766
39. Teng, Y. W., Mehedint, M. G., Garrow, T. A., and Zeisel, S. H. (2011) Deletion of murine betaine-homocysteine *S*-methyltransferase in mice perturbs choline and 1-carbon metabolism, resulting in fatty liver and hepatocellular carcinoma. *J. Biol. Chem.* **286,** 36258–36267
40. Fleming, T. P., Kwong, W. Y., Porter, R., Ursell, E., Fesenko, I., Wilkins, A., Miller, D. J., Watkins, A. J., and Eckert, J. J. (2004) The embryo and its future. *Biol. Reprod.* **71,** 1046–1054
41. Lucifero, D., Chaillet, J. R., and Trasler, J. M. (2004) Potential significance of genomic imprinting defects for reproduction and assisted reproductive technology. *Hum. Reprod. Update* **10,** 3–18
42. Harris, S. E., Gopichandran, N., Picton, H. M., Leese, H. J., and Orsi, N. M. (2005) Nutrient concentrations in murine follicular fluid and the female reproductive tract. *Theriogenology* **64,** 992–1006
43. Biggers, J. D., Lawitts, J. A., and Lechene, C. P. (1993) The protective action of betaine on the deleterious effects of NaCl on preimplantation mouse embryos *in vitro*. *Mol. Reprod. Dev.* **34,** 380–390
44. Anbari, K., and Schultz, R. M. (1993) Effect of sodium and betaine in culture media on development and relative rates of protein synthesis in preimplantation mouse embryos *in vitro*. *Mol. Reprod. Dev.* **35,** 24–28
45. Lawitts, J. A., and Biggers, J. D. (1993) Culture of preimplantation embryos. *Methods Enzymol.* **225,** 153–164